Thermionic Emission from Tungsten and Thoriated Tungsten Filaments

W. B. NOTTINGHAM, *George Eastman Research Laboratory of Physics, Massachusetts Institute of Technology, Cambridge, Massachusetts*

(Received October 7, 1935)

The electron emission from pure and thoriated tungsten filaments has been investigated as a function of the applied potential over the entire range from a few volts retarding to 1400 volts accelerating including careful studies at zero field. The filaments were heated with pulsating currents from thyratrons to eliminate during the measurements any drop in potential along the filament. The energy distribution of electrons was found to be deficient in slow electrons. An empirical reflection factor of $R(p_x)=\exp -p_x^2/2m\omega$, where ω is a constant 3.05×10^{-13} erg, represents the observed data for all temperatures and all states of activation for the thoriated tungsten. Analysis shows that there is no disagreement between the new results and the experiments of Germer. Zero-field Richardson plots show that the reflection effect alters both the A and b of Richardson's equation. The resulting values after correcting for reflection are $A=204$ and $b=55{,}100$ for pure tungsten. This value of A indicates a negative temperature coefficient of the work function of 4.3×10^{-5} volt per degree, which has been verified by an independent experiment. New data on the electron emission in accelerating fields are given for many states of activation, showing that there are large deviations from the Schottky mirror image theory. Becker's patch theory is discussed briefly and a simpler strip theory is developed which serves to represent the observed data as an empirical result. This analysis shows that the patch theory is not suitable to explain the reflection effect since it is independent of the state of activation of the filament.

INTRODUCTION

THE thermodynamic treatment of Dushman,[1] as well as the Fermi-Sommerfeld[2] theory of metals, yields the equation

$$I=(4\pi m\epsilon k^2/h^3)T^2e^{-b/T} \qquad (1)$$

for the saturation emission from an ideal emitting surface at zero field. The constants m, ϵ, k, and h have their usual significance and if values are introduced so as to express the current in amp. per cm², this coefficient has the value 120 amp. per cm² per degree.[2] Experiment shows that no known emitting surface meets the requirements of being an *ideal surface.* Real surfaces are defective in the following respects: (1) The true surface area is generally not equal to the apparent area. (2) The work function b which would be appropriate for a given small area of the surface (for example, a single crystal facet) is generally not the same over the entire surface used in experiment because of defects at crystal boundaries and because evaporation often exposes two or more kinds of crystal facets. Surface contaminations produce regions of different work functions. (3) Real surfaces generally show electron reflection effects. (4) Instead of the true work function b, we usually measure another quantity b_0 which may be related to b by the equation[3]

$$b=b_0+\alpha T. \qquad (2)$$

It is the purpose of this paper to present certain new experimental facts which may be interpreted in terms of these differences between real and ideal emitting surfaces. The method of attack was to study the electron emission as a function of the electric field over the entire range from a few volts of retarding potential to over 1400 volts accelerating potential for as wide a range of temperature as possible and for all states of activation when using a thoriated filament.

ELECTRON EMISSION FROM A FILAMENT IN A RETARDING ELECTRIC FIELD

Experimental tubes

For accurate measurements of emission in a retarding field or with very low accelerating fields, it is absolutely necessary that there be no drop in potential along the filament being studied. The filament must be long and the emission must be uniform over the entire length which is able to deliver current to the observing

[1] S. Dushman, Phys. Rev. **21**, 623 (1923). Original treatment did not include effect of electron spin which doubles the earlier value of 60 amp. per sq. cm per degree.

[2] L. Nordheim, Physik. Zeits. **30**, 177 (1929).

[3] Within the accuracy of present day experiments, only these two terms of the power series expansion are needed.

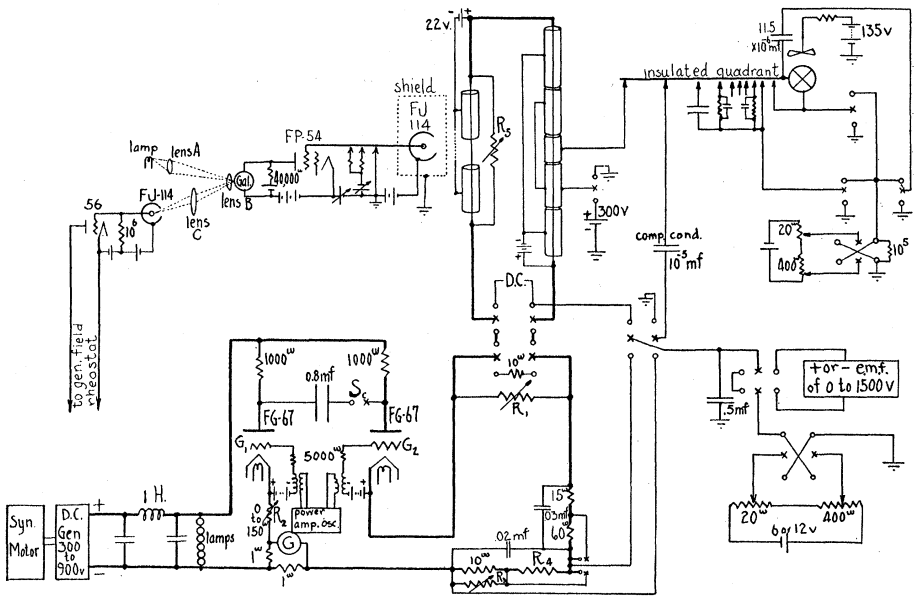

FIG. 1. Thyratron inverter circuit for heating filament with pulsating current.

instrument. The tubes used with thoriated tungsten filaments contained five tantalum collectors 1 cm in diameter, concentric with respect to the filament. The center collector, 2.5 cm long, was well insulated and served to deliver the electron current to the electrometer for measurement. The measuring circuit insured that this collector was always at ground potential. The two collectors adjacent to this one were 4.5 cm in length and were always maintained at ground potential. The two outermost collectors, also 4.5 cm in length, were generally maintained 12 volts negative with respect to the filament. This was done in order to suppress all electron emission from the ends of the filament which were never in the same condition as the middle because the temperature was lowered by the cooling effect of the leads and because the state of activation was very different from that at the middle. The filament material used is designated by the General Electric Company as "E" wire containing about one percent ThO_2 and no carbon. The filaments were about 21 cm in length and about 2.8 mils in diameter. The upper end of the filament was fixed while the lower end was held by a tungsten spring made in accordance with the information published by Langmuir and Blodgett.[4] The filament was welded to small "chips" of tantalum which in turn were welded to the supporting connections. Potential leads were also welded to these "chips" so that the true over-all potential of the filament could be measured accurately by a Leeds and Northrup type K potentiometer operated to give a 16-volt range instead of the usual maximum of 1.6 volts. The potential drop over a one-ohm resistance served to give an accurate measure of the filament current. The temperature of the filament was determined from these measurements after correction for end losses,[5] with both the Langmuir-Jones[6] and the Forsythe and Watson[7] temperature scales. Since these two scales yield temperatures which differ by about 3 to 5 degrees, a temperature was always taken lying between the two scales, generally a little nearer the F and W value. The temperatures were calculated from the functions, according to the Langmuir-Jones notation, $A/d^{\frac{3}{2}}$, $VA^{\frac{1}{2}}/l$ and

[4] Katharine B. Blodgett and I. Langmuir, Rev. Sci. Inst. **5**, 321 (1934).
[5] I. Langmuir, S. MacLane and K. B. Blodgett, Phys. Rev. **35**, 478 (1930).
[6] H. A. Jones and I. Langmuir, Gen. Elec. Rev. **30**, 310, 354, 408 (1927).
[7] W. E. Forsythe and E. M. Watson, J. Opt. Soc. Am. **24**, 114 (1934).

VA/ld. In terms of the resistivity R and the total watts W, these are $W^{\frac{1}{2}}/R^{\frac{1}{2}}$, $W^{\frac{3}{4}}R^{\frac{1}{4}}$ and W, respectively. In computing the final temperatures, the last two were given greater weight. When the filament was heated by pulsating current, the temperature was held constant within about 0.1 degree by a "photoelectric ammeter" which will be described below.

One of the tubes containing the pure tungsten wire (G. E. Co. 218) had only three collectors and consequently the results obtained are probably less reliable because of the shortness of the filament and the fact that impurities might have been present near the cool ends of the filament, giving an abnormal contribution to the emission. Another tube with a tungsten filament had five collectors as described above and also 0.6-mil potential leads welded directly to the filament at a distance far enough from the supporting leads so that the cooling effect could be neglected. In this tube the filament was not exactly on the axis of the collectors at all temperatures and therefore the results obtained in this case are subject to a little doubt, although calculation shows that the effect of noncentering should be of secondary importance.

An extensive outgassing schedule was used in every case, lasting between three and five days. All metal parts were outgassed before assembly and the cylinders were heated many hours at a high temperature by induction after the final assembly. Oven baking at 450°C was used. Before sealing off, two or three magnesium-barium getter caps were heated lightly to give a deposit of "getter" over the lower end of the tube. After heating the getter caps and also the seal-off constriction, the collectors were heated extensively by electron bombardment just before the final seal-off of the tube. Ionization current measurements were made by connecting the center collector to a potential 22 volts negative with respect to the filament and the two adjacent collectors to 220 volts positive with respect to the filament. The electron current to ion current ratio was generally about 10^7 to one. Although this corresponds to a pressure of about 10^{-8} mm of mercury, the fact that the condition of the filament would remain very accurately constant for weeks at a time without high temperature flashing proved that the partial pressure of any gas which could contaminate the filament had been reduced to a very small fraction of that indicated by the ionization current measurements. Early in the outgassing process the filament was heated to at least 3000°K for ten seconds and maintained at somewhat lower temperatures for some hours to remove the traces of impurities which so greatly distort results if this is not done.

Electric circuits

The filament heating circuit was patterned after the one described in a previous publication,[8] which will be referred to below as (PR–I). Certain improvements which make for a considerable increase in accuracy necessitate the reproduction of the circuit diagram in its modified form. Although one can see by an inspection of the diagram the main features, some of the others need explanation.

The galvanometer G gave a continuous indication that the heating current was on exactly one-half of the time. This was accomplished by first adjusting the resistance R_1 to give the correct heating current through the filament after which the switch S_c was opened so as to cause both thyratrons to remain on continuously. R_2 was then adjusted to bring about a "static" balance, as indicated by the galvanometer G. The resistances of the two branches of the circuit were thus equalized to better than 0.1 percent. With switch S_c closed, the 200-cycle oscillator input to the grids G_1 and G_2 was adjusted to give a "dynamic" balance as indicated by the galvanometer. After this was done, a check of the thermionic current, with an accelerating field high enough so that the drop in potential along the filament when heated by direct current was negligible, showed that the electron current delivered with pulsating heating current was accurately one-half that observed with d.c. heating.

Because of the fact that dielectrics are never perfect, compensation was necessary to eliminate the capacity currents which would otherwise flow in and out of the collector system because of the large changes of potential of the filament with respect to the collector as the heating current

[8] W. B. Nottingham, Phys. Rev. **41**, 793 (1932).

went on and off. In the extreme cases, this was as much as 75 volts. The compensation was accomplished by putting on a retarding potential V of about 6 volts, so as to cut off all electron emission, after which the ground key was opened while the electrometer circuit was arranged for the highest sensitivity. If the compensation was not correct, a throw to the right or left was observed, depending on whether the ground key was opened during a heating or nonheating cycle. By adjusting rheostat R_3 and resistance R_4 this throw was eliminated, thus showing perfect compensation.

For the smallest currents the rate of charging a condenser was used for the measurement. The condensers used were 11.5×10^{-12} farad and 403×10^{-12} farad, the smaller being mounted as part of the electrometer, while the latter was a quartz insulated 25-plate fixed condenser which also served as a standard for calibrating the high resistances used when the range of electron currents measured was so small that the one megohm standard could not be used satisfactorily. These condensers permitted the measurement of currents of 5×10^{-15} amp. to an accuracy of about 2 percent. The electrometer sensitivity was 6 mm per millivolt, and it was adjusted to be very slightly under-damped with a period of about 4 sec. The electrometer was of the Compton type of our own design with a needle of 2.5 mm radius.

Resistances between 6 and 5000 megohms were made by evaporating platinum in high vacuum on the inside of Pyrex bulbs. These, as well as wire wound resistances from 100 ohms to one megohm, were used for measuring the high currents. In every case the resistances were shunted by capacities such that the time constant CR was of the order of 0.6 sec. This is necessary in order that the collector potential remain essentially at ground potential as indicated by the balance of the electrometer, otherwise the collector will go negative with respect to ground about half the voltage required to give the compensation.

A General Electric FJ-114 photo-cell was used with the "photoelectric ammeter." Since this tube changed its sensitivity slowly after changes in illumination, it was kept under a constant state illumination continuously. The shunting resistance R_5 permitted the use of a constant current through the auxiliary filament. The output of the photo-cell was measured by a null method using an FP-54 amplifier. Thus the zero reading of the galvanometer in the plate circuit served as a continuous indication of the filament temperature. The sensitivity was such that a six to ten-cm deflection was produced by a one-degree change in temperature of the filament. While one galvanometer lamp was used to indicate the deflection, a second one was used for automatic compensation. The image of the condensing lens A of the galvanometer lamp was brought to focus by the galvanometer lens B on a large reading glass lens C fitted with a wedge-shaped aperture. This lens focused the image of the lamp filament on a FJ-114 photo-cell which controlled the plate current of a 56 type vacuum tube shunted across the field rheostat of the generator. By adjusting the intensity of the lamp, the system could be made to compensate almost perfectly for all rapid changes in the filament heating circuit due to changes in the power line voltage or frequency. This continuous temperature indication and automatic adjustment supplemented by manual control was absolutely essential for obtaining accurate results. Even though the absolute temperature is not known to better than two or three degrees, the temperature must be maintained *constant* to within a tenth of a degree because the emission change with the temperature corresponds to between the thirtieth and the fortieth power.

Experimental results

The curves of Fig. 2 illustrate in a qualitative way the sort of results one obtains for a thoriated filament at various states of activation. The energy distributions are all alike independent of the state of activation, and the contact potential shifts with changes in activation in the expected way. It is not difficult to determine zero field from these data when plotted on a much larger scale and fitted by a computed curve as is illustrated by Fig. 3. The applied potential at zero field is shown on each curve by a short vertical mark. Theoretically these zero-field points should have fallen on a straight line the slope of which is shown by the dotted straight line marked "theory." The fact that these points

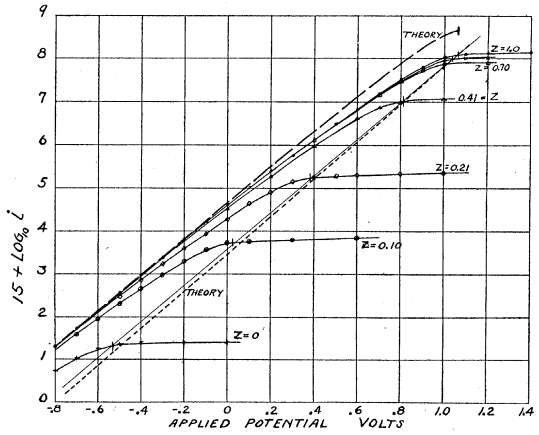

FIG. 2. Electron energy distributions from a thoriated filament for different states of activation. $T=1160°K$. Short vertical lines joined by light weight solid line show zero-field points. Dotted line shows theoretical slope of zero-field line. Dashed line shows theoretical energy distribution for $Z=1.0$ computed for cylinders and assuming no reflection.

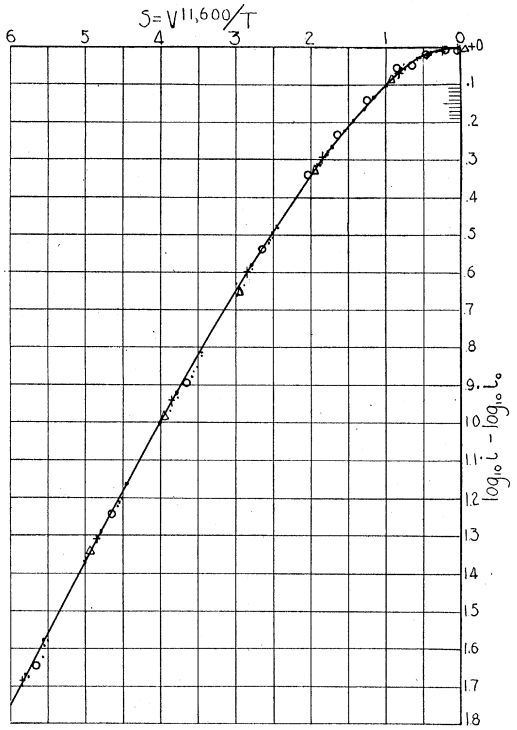

FIG. 3. Composite of electron energy distributions for nine states of activation. Circle, $Z=0.046$; cross, $Z=0.25$; triangle, $Z=1.3$. Line computed with $k/\omega=4.5\times10^{-4}$. i_0=current at zero field. $T=1160°K$.

do not fall exactly on the dotted theoretical line may be attributed to the rather unfamiliar effect* that the work function of a collector as indicated by its contact potential increases as a result of the flow of a large current of slow electrons. The flow of electrons with an energy of 50 electron volts or more produces the opposite effect. The time required for the collector to recover from such effects lasts for some minutes or even hours in the case of nickel collectors which have received considerable thorium. The time of recovery for clean tantalum collectors is less than the time required for measurement. Time lag effects have also been observed by Millikan,[9] Germer,[10] Mönch,[11] and Nottingham.[12]

It is important to notice that the curves *do not* follow the theoretical energy distribution curve, shown by the dashed line of Fig. 2. This is calculated assuming that the electrons have a Fermi-Dirac distribution within the metal and have a transmission coefficient of unity. The natural conclusion, of course, is that there is some mechanism producing reflection at the surface with the result that part of the slow electrons are not emitted. The distribution curve (PR–I, Fig. 6), obtained under much less satisfactory vacuum conditions, showed even more marked deviations from the theoretical curve. It is now known that the early results apply to a complex composite surface containing probably a layer of oxygen underlying the layer of thorium. The form of the potential barrier, shown PR–I, Fig. 13 and proposed as an explanation of the experimental results, seems to be reasonable if one recognizes that the "hump" assumed is due to the oxygen layer plus the thorium layer and not due to a thorium layer alone, as was originally thought. If the vacuum conditions are sufficiently perfect, this "post activated state"[13] is

* Dr. Irving Langmuir insists that this phenomenon should have a name. The author therefore suggests that it be called the "anode effect."

[9] R. A. Millikan, Phys. Rev. **18**, 236 (1921).

[10] L. H. Germer, Phys. Rev. **25**, 795 (1925).

[11] Günther Mönch, Zeits. f. Physik **65**, 233 (1930); W. Leo, Ann. d. Physik **9**, 347 (1931).

[12] W. B. Nottingham, Phys. Rev. **39**, 183 (1932).

[13] A thoriated filament may be activated, after the proper preliminary heat treatment, at a temperature of about 1920°K, for example, and the emission will increase as is illustrated in PR-I, Fig. 5. One may refer to the state of coverage which gives the maximum emission for strong fields as "$f=1.0$" as proposed by Brattain and Becker (Phys. Rev. **43**, 428 (1933)), or one may describe the coverage as in this paper by a "Z" scale, defining $Z=1.0$ as that coverage giving the maximum emission at zero field. The objection to the "f" scale is its dependence upon the

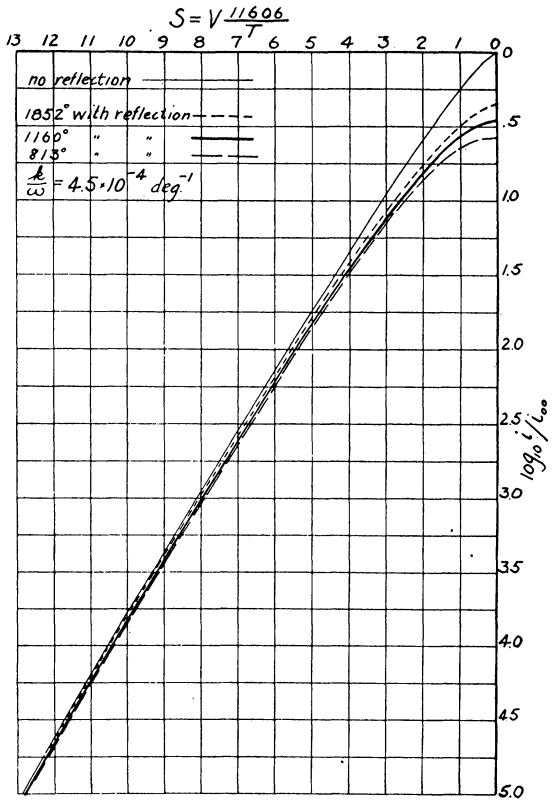

FIG. 4. Computed energy distributions.

not produced, and the distribution curves are not essentially different from those obtained for pure tungsten.

surface field. With a field of about 6000 volts per cm we find $f=1.5Z$. If the activation is carried on at 1800°K or lower, and the time required to produce the various states of activation noted, then Z is defined as $Z\equiv t/t_m$ where t_m is the time required to activate to the maximum zero-field emission. This assumes that the average rate of arrival of thorium atoms on the surface is constant and that no evaporation takes place. These "f" or "Z" scales must be recognized as temporary. We need a "θ" scale which measures the true fraction of the surface covered. After having activated to a coverage of $Z=1$ or more, if the vacuum conditions are not "perfect," the emission may increase two- to six-fold even though the filament is cold between test readings. We have used the term "post-activation" to describe this increase in emission. As post-activation progresses, one observes that the emission passes through a maximum after which the emission decreases indefinitely until it practically disappears. A flash for less than a minute at 1850 not only removes the effect of post-activation, but if it has progressed far enough to give the maximum emission, practically the entire coating leaves the filament and it must be reactivated before even "normal" emission is obtained. The filament condition for most of the work reported in PR-I corresponded to that state of the filament for which the maximum emission occurred with post-activation. In the tubes studied for the present investigation, the vacuum conditions were so good that no detectable post-activation took place in a month's time.

Fig. 3 serves to illustrate the fact that the form of the energy distribution is independent of the state of activation. Eighty-five points taken at nine different states of activation were used to make up this composite curve. The three states of activation of particular interest are $Z=0.046$, $Z=0.25$ and $Z=1.3$ when considered from the standpoint of a patch theory. These points are identified by circle, cross and triangle, respectively. The extent to which these experimental data deviate from the expected Fermi (or Maxwellian) distribution is illustrated in Fig. 4, in connection with the theory of reflection which follows.

Theory of collection in a retarding field

There are two possible mechanisms which might produce reflection of electrons at an emitting surface. There is the possibility that reflection takes place due to the periodic structure of the metal lattice and the wave properties of electrons. This problem has been treated by Nordheim[14] and by Frank and Young[15] by approximate methods neglecting any possible effect of the crystal lattice with the result that a reflection of about 6 percent is expected for low energy electrons. As the energy of the emerging electrons increases to a number of volts, this reflection coefficient decreases very gradually. (See Fig. 21.) The nature of the curve is such that the effect could not be detected in the energy distribution of the electrons and would only show up as a five percent decrease in the total emission. Such a small effect would be masked by other things and therefore the theory could only be tested by shooting a beam of very slow electrons on the surface. Thus, the quantum theory as applied in the approximate form to the problem of reflection at the surface of a metal does not show promise of explaining the observed fact that the energy distribution has a shortage of low energy electrons as was seen above.

A second possibility is that the surface inhomogeneities such as work function differences between facets of a single crystal might produce potential hills of such a nature that reflection might be produced. It is a well-known

[14] L. Nordheim, Proc. Roy. Soc. **A121**, 626 (1928).
[15] N. H. Frank and L. A. Young, Phys. Rev. **38**, 80 (1931).

experimental fact that the emission from a composite surface such as thoriated tungsten, or caesium covered tungsten, changes greatly with the accelerating field if the surface is only partly covered. Langmuir and Compton[16] proposed a checkerboard patch theory to account for this effect. Becker[17] has also applied this sort of theory to emission in accelerating fields and has pointed out that patches would cause a reflection effect. The difficulty with this explanation of reflection is that throughout the entire range of activation from $Z=0.01$ to $Z=1.4$, the energy distributions are *exactly alike* indicating that whatever causes the reflection, it is *independent* of the state of activation of the surface.

Since it is not practical to work with anything but a cylindrical or filament type of emitter for accurate work, it is necessary to work out the method by which observed data taken with concentric cylinders can be correctly interpreted in terms of a reflection coefficient depending on the energy of the electron as it leaves the filament. A very simple form of reflection coefficient is the exponential type given by

$$R(p_x)=e^{-p_x^2/2m\omega}, \tag{3}$$

where ω is a constant and p_x is the momentum in the direction perpendicular to the surface in excess of that required to carry the electron to infinity when there is no external electrostatic field in the space, i.e., with "zero field." Thus, as the excess momentum approaches zero, the reflection approaches unity, while for large values of p_x the reflection goes to zero exponentially at a rate which depends on ω.

For an electron to arrive at a cylindrical collector, it must leave the emitting filament with enough radial and tangential momentum to overcome the retarding potential. The energy and momentum equations yield at once the limiting relationship

$$p_x^2+p_y^2(1-r^2/R^2)=2m\epsilon V, \tag{4}$$

where p_x and p_y are the radial and tangential momentum components just outside the filament, as defined more carefully above. Since the collector radius R is generally much larger than the filament radius r, Eq. (4) reduces simply to $p_x^2+p_y^2=2m\epsilon V$. Using the Fermi-Sommerfeld theory of metals we can write the expression for the emission current received by a cylindrical collector with a retarding potential V.

$$i=\frac{2\epsilon}{h^3}e^{-(W_a-W_i)/kT}\int_{p_z=-\infty}^{p_z=+\infty}\int^{p_y=\infty}\int^{p_x=\infty}(1-e^{-p_x^2/2m\omega})(p_x/m)e^{-(p_x^2+p_y^2+p_z^2)/2mkT}dp_x dp_y dp_z, \tag{5}$$

where $(W_a-W_i)/k$ is the same as b of Eq. (1). The limits of integration with respect to p_x and p_y exclude the region inside of the semicircle $p_x^2+p_y^2=2m\epsilon V$ but otherwise include the region of p_x from 0 to ∞, and of p_y from $-\infty$ to $+\infty$. The integration of Eq. (5) gives

$$i=i_{00}\{G(S)-F(S, kT/\omega)\}, \tag{6}$$

where

$$i_{00}\equiv(4\pi m\epsilon k^2/h^3)T^2e^{-(W_a-W_i)/kT}, \tag{7}$$

$S\equiv v(11{,}600/T)$, with v the retarding potential in volts.

$$G(S)\equiv(2/\sqrt{\pi})S^{\frac{1}{2}}e^{-S}+1-(2/\sqrt{\pi})\int_0^{S^{\frac{1}{2}}}e^{-x^2}dx, \tag{8}$$

$$F(S, kT/\omega)\equiv\frac{1}{1+kT/\omega}\left\{\left(\frac{\omega}{kT}\right)^{\frac{1}{2}}\frac{2}{\sqrt{\pi}}e^{-S(1+kT/\omega)}\int_0^{(SkT/\omega)^{\frac{1}{2}}}e^{y^2}dy+1-\frac{2}{\sqrt{\pi}}\int_0^{S^{\frac{1}{2}}}e^{-x^2}dx\right\}. \tag{9}$$

With the help of the Jahnke and Emde tables, $F(S, kT/\omega)$ was computed for various values[18] of (kT/ω) and selected values of S. Table I gives the results of this calculation in sufficient detail

[16] K. T. Compton and I. Langmuir, Rev. Mod. Phys. **2**, 123 (1930).

[17] J. A. Becker, Rev. Mod. Phys. **7**, 95 (1935).

[18] For $SkT/\omega>4$ the form of $F(S)$ given in Eq. (9) is not as convenient as the following:

TABLE I. *Values of $F(S, kT/\omega)$ for various values of S and kT/ω* (see Eq. (9)).

S	0	0.5	1	1.5	2	3	4	5	6	8	10
kT/ω											
0	1.0	8.01^{-1}	5.72^{-1}	3.91^{-1}	26.1^{-2}	11.2^{-2}	4.6^{-2}	18.6^{-3}	7.38^{-3}	11.3^{-4}	17^{-5}
0.06	0.943	7.47	5.25	3.51	23.1	9.5	3.78	14.3	5.62	8.4	11.8
.12	.893	6.98	4.83	3.18	20.5	8.14	3.12	11.7	4.35	6.05	7.9
.20	.833	6.41	4.31	2.81	17.7	6.75	2.45	8.85	3.20	3.99	5.00
.40	.714	5.30	3.42	2.09	12.6	4.39	1.47	5.00	1.75	1.96	2.33
.60	.625	4.47	2.75	1.62	9.12	2.69	0.974	3.21	1.00	1.12	1.25
.80	.556	3.86	2.28	1.29	7.23	2.25	.70	2.29	0.66	0.751	0.873
1.0	.500	3.38	1.90	1.05	5.13	1.73	.538	1.62	.502	.578	.672
1.2	.455	2.95	1.63	0.872	5.00	1.41	.401	1.28	.450	.461	.552
1.4	.417	2.62	1.40	.739	4.00	1.19	.331	1.06	.40	.386	.470
1.6	.385	2.34	1.23		3.37						
2.0	.337	1.92	0.959		2.61	0.718					
3.0	.250	1.29	.611		1.54	.453	.143				
5.0	.167	0.735	.325		0.879						

Note 1. The row for $kT/\omega=0$ is $G(S)$ since the first term of Eq. (9) reduces to $2S^{1/2}e^{-S}/\sqrt{\pi}$ in the limit.
Note 2. The superscript at the top of each column indicates the power of ten by which the numbers in that column should be multiplied.

for interpolation curves to be plotted by the user so that the theoretical curves for a limited range of values of (kT/ω) may be produced readily.

It was the original intention at the time these computations were made simply to "translate" observed curves such as those shown in Figs. 2 and 3 into corresponding transmission or reflection curves. For that reason, a method was worked out to evaluate the three constants of the following equation

$$R(p_x)=(1-f)e^{-p_x^2/2m\omega_1}+fe^{-p_x^2/2m\omega_2} \qquad (10)$$

and thus make the empirical curve pass through three points of the observed curve. Here ω_1 and ω_2 are constants and f is a constant less than unity. All three constants are to be selected best to fit the data as an empirical equation. To do this, one chooses the three values of S at which the experimental and the empirical curves are to intersect. The ones selected were $S=0$, 2 and 6. Two curves were made by plotting $F(0, kT/\omega)$ as the abscissa and $F(2, kT/\omega)$ as the ordinate for one, while $F(0, kT/\omega)$ and $F(6, kT/\omega)$ were used for the abscissa and ordinate of the second. Since $F(S, kT/\omega)$ measures the amount the calculated curve falls below the Maxwellian curve $G(S)$, the experimental values of the deficiency may be called $E(S)$ and plotted as points $(E(0), E(2))$ and $(E(0), E(6))$ on the two graphs described above. If a straight line can be found which passes through the E points intersecting the F curves so as to give common values of $F(0, kT/\omega_1)$ and $F(0, kT/\omega_2)$ for the two curves, then two of the constants, *viz.*, ω_1 and ω_2, will have been determined. If such common values do not exist, then the empirical curve cannot be made to pass through the three experimental points selected. The third constant is given by the equation

$$f=\frac{F(0, kT/\omega_1)-E_0}{F(0, kT/\omega_1)-F(0, kT/\omega_2)}. \qquad (11)$$

When this method was applied to the experimental data shown in Fig. 3, the points $(E(0), E(2))$ and $(E(0), E(6))$ fell exactly on their respective lines at a common value of $F(0, kT/\omega)$ thus giving $kT/\omega_1=kT/\omega_2$ and showing that the simple one constant expression of Eq. (3) represents the experimental data with accuracy. The solid line of Fig. 3 is the computed curve using $k/\omega=4.5\times10^{-4}$ degree^{-1}. This value of ω is 3.05×10^{-13} erg or 0.191 electron volt. The three curves of Fig. 4 are computed for the temperatures 813°K, 1160°K and 1852°K as indicated.

$$F(S, kT/\omega)=\frac{1}{1+kT/\omega}\left\{\frac{2}{\sqrt{\pi}}\frac{e^{-S}}{(kT/\omega)^{\frac{1}{2}}}f(a)+1-\frac{2}{\sqrt{\pi}}\int_0^{S^{\frac{1}{2}}}e^{-x^2}dx\right\},$$

where $a\equiv SkT/\omega$ and $A\equiv(a/(a-1))^{\frac{1}{2}}$,

$$f(a)\equiv[A/a-e^{-a}\{(A+0.312)/a+(A-1.25)+(a/2)(A-1)\}].$$

A short table of values of $2f(a)/\sqrt{\pi}$ follows.

a	3	4	5	6	7	
$(2/\sqrt{\pi})f(a)$	0.403	0.307	0.249	0.205	0.1735	
a	8	9	10	12	14	16
$(2/\sqrt{\pi})f(a)$	0.1506	0.133	0.119	0.0986	0.0837	0.0728
a	18	20	21	24	27	30
$(2/\sqrt{\pi})f(a)$	0.0645	0.0579	0.055	0.0481	0.0426	0.0382

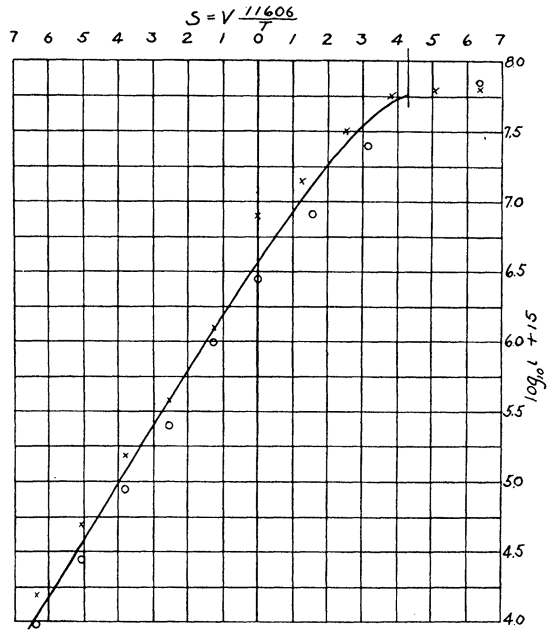

FIG. 5. Germer's data on electron energy distribution for $T=1830°K$. Curve computed with $k/\omega=4.5\times10^{-4}$ deg.$^{-1}$. Circles, increasing retarding potentials; crosses, decreasing potential.

All data observed at all states of activation and all temperatures using the thoriated filament were found to be accurately represented with the single reflection constant of $(k/\omega)=4.5\times10^{-4}$ deg.$^{-1}$. This same coefficient also represented the observed results for pure tungsten filaments almost as perfectly. This qualification is necessary because the fit was not quite perfect and it remains to be determined with an improved experimental tube whether or not there is a real difference in the reflection curve of pure tungsten as compared with thoriated tungsten.

As was stated above, the mechanism for producing this reflection is as yet undetermined, but the fact that there is a reflection effect seems to be established. The work previously quoted as the best authority for the fact that electrons are emitted with a Maxwellian distribution of energies and that no reflection takes place is that of Germer.[19]

Fig. 5 is produced here to show that there is no conflict between Germer's data and the reflection hypothesis. Here Germer's experimental points are shown and the curve drawn was computed, using $(k/\omega)=4.5\times10^{-4}$. The circles represent the observations made with increasing retarding potentials, while the crosses correspond to the series taken with decreasing retarding potentials.

[19] L. H. Germer, Phys. Rev. **25**, 795 (1925).

Reflection interpreted as excluded areas

According to the patch theory, which is discussed below, we might interpret the reflection in terms of a nonuniform transmission of electrons as a function of the coordinates of the surface. From the observed energy distribution data above, it is possible to construct a picture which shows essentially the fraction of the surface which should be allotted to transmission and reflection as a function of the energy. In Fig. 6 the cross-hatched part indicates a reflection, while the remainder represents the transmission. Thus, at any specified energy level ϵ_x a horizontal line started at $z=0$ passes through shaded territory for part of its length and nonshaded territory for other parts of its length. If we consider a segment of such a line of unit length, the fraction of it found in the shaded part of the figure measures the reflection coefficient, while the fraction in the nonshaded part measures the transmission. The figure is made up by repeating the line given by $\epsilon_x=2.3\omega\log_{10}z_0/2z$ where $\omega=0.191$ electron volt, the value shown above to fit the experimental data, and z, which is directly proportional to the area of the excluded region, takes on values between zero and $z_0/2$. The distance between adjacent peaks is taken as z_0 in order to fit in with the patch theory discussion below. For an energy of $\epsilon_x=0.2$ electron volt, 35 percent of the surface area would be assumed to be nonemitting, according to this interpretation. The object in presenting this figure is to show the kind of selectivity which

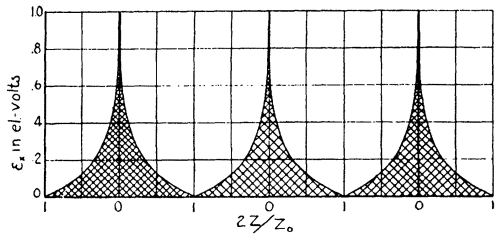

FIG. 6. Pictorial representation of reflection and transmission properties of a surface. $\epsilon_x\equiv P_x^2/2m$.

a patch theory would have to exhibit in order to be consistent with the experimental data. Since the analysis below indicates that patch theories are not likely to give effects of this kind, it might be worth while to investigate theoretically the possibility that the surface layer of atoms is responsible for the reflection effect in which case z_0 would be the interatomic distance.

Zero-Field Richardson Plots

Since the entire energy distribution curve can be fitted so accurately by a computed curve, there is no difficulty in establishing zero field and therefore the emission which would have been observed in the absence of reflection is easily computed. At zero field Eq. (6) reduces to

$$i_0 = i_{00}\left(1-\frac{1}{1+kT/\omega}\right) = i_{00}\left(\frac{1}{T_\omega/T+1}\right), \quad (12)$$

where T_ω is defined by $T_\omega \equiv \omega/k$ and i_{00} is the emission which would have been observed at zero field with no reflection. Thus, after observing i_0, we can compute i_{00} at once. The zero-field emission should be uninfluenced by surface excess effects and also patch effects, since these will be absorbed in the reflection coefficient if they have any influence on the zero-field emission. This leaves only the temperature coefficient of the work function as an undetermined factor, and one may write

$$\log_{10}(i_{00}/T^2) = \log_{10} 120 - 0.4343\alpha - 0.4343(b_0/T). \quad (13)$$

We plot $\log_{10}(i_{00}/T^2)$ as a function of $(1/T)$ as in Fig. 7.

The slope of the upper straight line gives the work function at 0°K as defined by Eq. (2) and the intercept or the observed value of $\log_{10} A$ (according to the usual notation) allows us to calculate α as

$$\alpha = 2.3(\log_{10} 120 - \log_{10} A). \quad (14)$$

The lower straight line of Fig. 7 represents the observed emission at zero field i_0. Both curves have been plotted to show that in either case the Richardson line is straight within the experimental error. The largest error is in the temperature scale and can be reduced only by making an accurate scale for the particular filament being used.

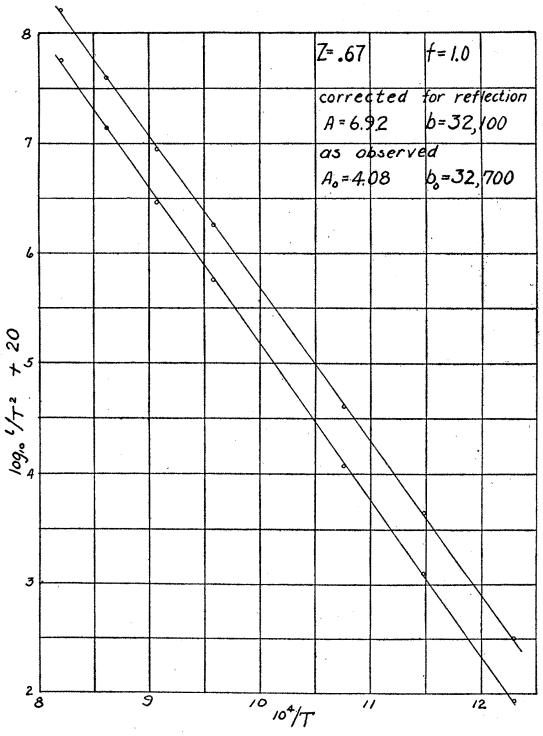

FIG. 7. Zero-field Richardson plots for a thoriated filament $Z=0.67$. Upper line includes correction for reflection.

The reflection effect not only alters the value of A, but also the value of b. By plotting $\log_{10}(T_\omega/T+1)^{-1}$ against $1/T$ for a particular range of observation, we may find the approximate correction to the A and the b brought about by the reflection. Richardson plots were made like Fig. 7 for $Z=0.67$, 1.0 and 1.3, but it was found impractical to attempt it for values of Z less than 0.67 on account of the changes which took place in the surface with the time. The existence of the effect is illustrated by the curves shown in Figs. 8 and 9. The heavy line of Fig. 8 shows a Schottky plot for Z approximately 0.1 and a temperature of 1160°K after ten hours heating at 1160°K. After heating the filament for three minutes at 1435°K, the emission at 100 volts was observed to have dropped to less than half its original value after which it returned to "normal" in about three hours time at 1160°K. The light line of Fig. 8 shows the shape of the

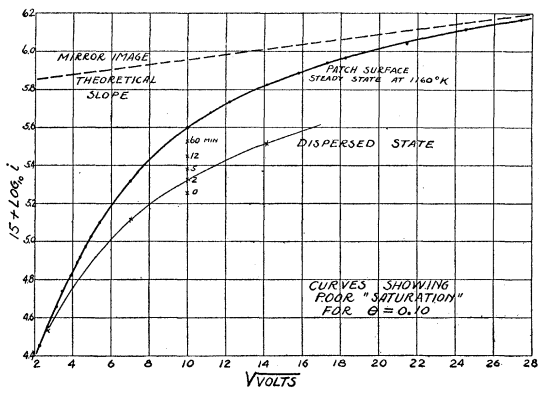

FIG. 8. Schottky curves for a thoriated filament. $T=1160$.

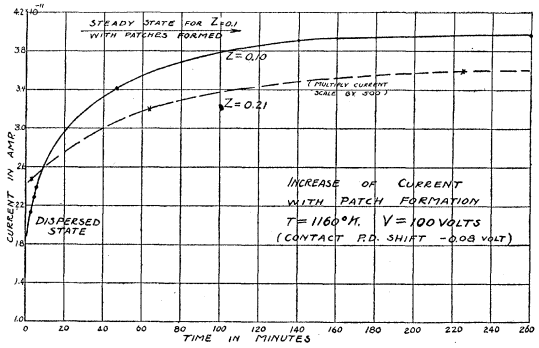

FIG. 9. Increase of current with patch formation.

curve two minutes after the high temperature treatment. Any form of patch theory suggests at once that the steady state at 1160°K corresponds to a more patchy state than that at 1435°K which we chose to call a "dispersed" state. With the patch state we have regions of relatively low work function which give a high emission with the help of a strong field, but at the same time the *average dipole moment* per unit area of the whole filament is actually less in the patch state than it is in the dispersed state. This is to be expected from Langmuir's[20] deductions that there is a depolarizing effect of the thorium atoms on each other. The emission at zero field is a direct measure of the average dipole moment per unit area and this has been found experimentally to follow the expected course, i.e., as the patch is formed the zero-field emission *decreases*, while the strong field emission *increases* as shown above. Fig. 9 shows the change in current with the time for the two states of activation $Z=0.1$ and $Z=0.21$.

After having produced the dispersed state at some relatively high temperature, it may be maintained for fairly long periods of time if the temperature is not raised above 925°K.

Richardson constants were computed from two observations for the values of Z less than 0.67. The filament surface was conditioned by maintaining it some hours at the highest temperature at which zero-field emission was not limited by space charge for the higher states of activation* and then the temperature was dropped to that for which the zero-field emission was about 5×10^{-14} amp. At these two temperatures energy distribution and Schottky plot data were taken, so that the emission at zero field could be determined accurately. After making the reflection correction, Richardson's A and b were computed. The results are summarized by Figs. 10, 11 and 12.

There are three important points to notice in Fig. 10. First, the observed points fall on a smooth curve which is not a straight line, showing that the temperature coefficient is not directly proportional to the average dipole moment (or the work function change) as has often been thought to be true from strong field measurements. Secondly, the point observed on a pure tungsten filament falls very naturally on the line as indicated by the double circle. This must be taken as provisional, however, because of the tube limitations described above. Thirdly, we see that the A thus observed is greater than 120, which suggests that the temperature coefficient of the zero-field work function for pure tungsten is *negative*,[21] contrary to Becker's[22] assumptions based on strong field data.

[20] I. Langmuir, J. Am. Chem. Soc. **54**, 2798 (1932).

* For low states of activation, 1393°K was selected as the maximum temperature. At temperatures much higher than this, measurable activation took place during the time of measurement.

[21] P. W. Bridgman in his *Thermodynamics of Electrical Phenomena in Metals* (Macmillan, New York, 1934), p. 100, shows that if the entropy of the surface charge at 0°K is not zero, the effect on the emission would be indistinguishable from a negative temperature coefficient of the work function. According to the Fermi-Sommerfeld model for a metal, the pressure of an electron gas in equilibrium with a metal of work function $b\equiv(W_a-W_i)/k$ should be

$$p=(4\pi m\epsilon k^2/h^3)(k/2\pi m)^{1/2}\,T^{5/2}\exp(-b/T).$$

The latent heat per electron η as given by the Clapeyron equation is related to b as follows:

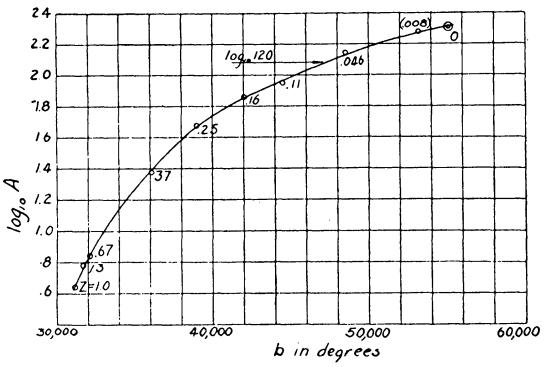

FIG. 10. Relation between $\log_{10} A$ and the zero-field work function from zero-field data corrected for reflection using $k/\omega = 4.5 \times 10^{-4}$ deg.$^{-1}$.

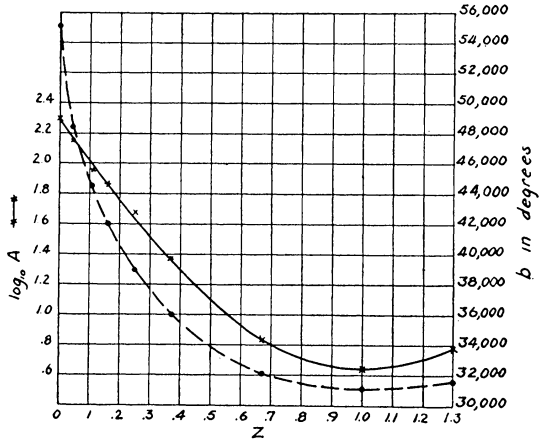

FIG. 11. $\text{Log}_{10} A$ (solid line) and b_0 as a function of Z after correction for reflection ($0.67f = Z$).

Fig. 11 shows the relation between $\log_{10} A$ and Z by the solid line while the dashed line relates

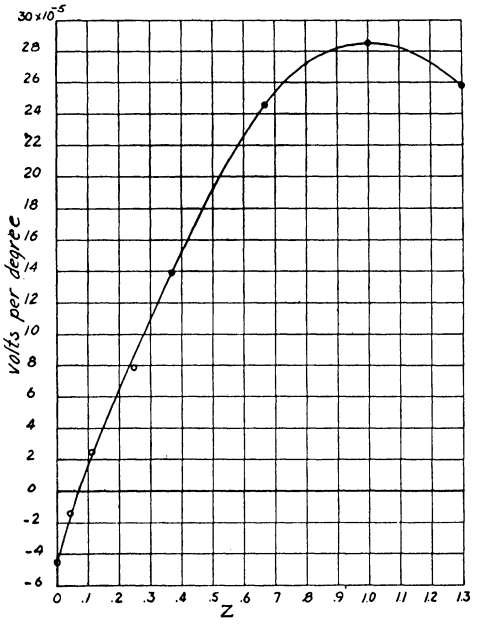

FIG. 12. Temperature coefficient of the work function as computed from log A.

b to Z. The surprise brought out by this curve is that both log A and b pass through a minimum at $Z = 1$. It was to be expected that b should pass through a minimum for about this coverage, but not so for log A.

These data translated in terms of the temperature coefficient of the work function by Eq. (14) are illustrated by Fig. 12.

Here we see that the temperature coefficient for pure tungsten seems to be -4.3×10^{-5} volt per degree. The work function thus *decreases* as the temperature increases. D. B. Langmuir has investigated this point by a direct experiment using an improved Langmuir-Kingdon[23] method over the range of temperature 350°K to 1050°K and obtains results which agree in sign and order of magnitude with this value. The method involved the measurement of the contact potential of the tungsten filament used as a collector and not as an emitter. This result is so important if true that we are not satisfied with the present experiments and expect to redetermine these constants with improved apparatus.

$$\eta = kT^2 \partial(\ln p)/\partial T = (5/2)kT + kb - kT(\partial b/\partial T).$$

We recognize $(5/2)k$ as the atomic heat of an ideal gas at constant pressure and can therefore write for the slope of the Richardson line,

$$\eta - (5/2)kT = \eta_0 - \phi(T) = kb - kT(\partial b/\partial T)$$

where η_0 is the latent heat at 0°K and $\phi(T)$ is determined by the heat absorbed in the metal due to the specific heat of the electrons and of the surface charge. The slope of a Richardson line such as that of Fig. 7 is constant within the experimental error. Therefore $\phi(T)$ is experimentally negligible compared to η_0. Within these limitations, $(\partial b/\partial T)$ must be a constant independent of the temperature and it follows that $kb_0 = \eta_0$. The temperature coefficient of the *work function* b may be *positive* or *negative* without conflicting with thermodynamic relationships.

[22] J. A. Becker and W. H. Brattain, Phys. Rev. **45**, 694 (1934). It should be emphasized that temperature coefficients cannot properly be calculated from strong field data without detailed knowledge of the surface structure.

[23] I. Langmuir and K. H. Kingdon, Phys. Rev. **34**, 129 (1929).

ELECTRON EMISSION IN AN ACCELERATING FIELD

Test of Schottky theory with pure tungsten and fully activated thoriated tungsten

The Schottky mirror image theory[24] predicts that the electron current from a hot filament should increase according to the equation

$$\log_{10} i_V = \log_{10} i_0 + 1.905(fV)^{\frac{1}{2}}/T, \qquad (15)$$

where for cylinders $f=(r \ln R/r)^{-1}$ with r and R the filament and collector radii, respectively. If the filament were perfectly smooth and the image force the only one acting on the electron at distances large compared with interatomic distances, then Eq. (15) should be accurate from voltages less than 2×10^{-3} volt to many thousand volts for ordinary sized filaments. The fact that the image law applies strictly for an infinite plane becomes a limitation only for voltages between zero and one millivolt. Experiment however shows that the current rises as predicted by the Schottky theory only for fields higher than 500 volts per cm.

According to Eq. (15), if we plot $\log_{10} i_V$ (i_V = observed current with the accelerating voltage V)* as a function of $11{,}600V^{\frac{1}{2}}/T$ the slope of the theoretical line should be $1.64\times10^{-4}f^{\frac{1}{2}}$. We see from Fig. 13 that this is true for the higher voltages since the straight line drawn with this slope fits the experimental points accurately. As the field is lowered the departure from the Schottky theory becomes more and more marked. That this is not an effect due to space charge is proven by Fig. 14, in which the departure from theory, plotted as a function of the voltage, is seen to be *greater the lower the temperature.*

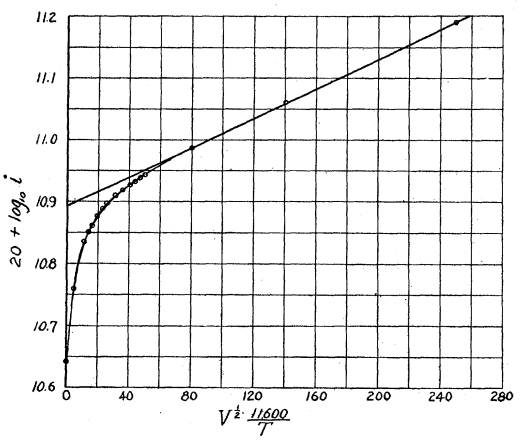

FIG. 13. Schottky plot for pure tungsten. $T=1434$°K.

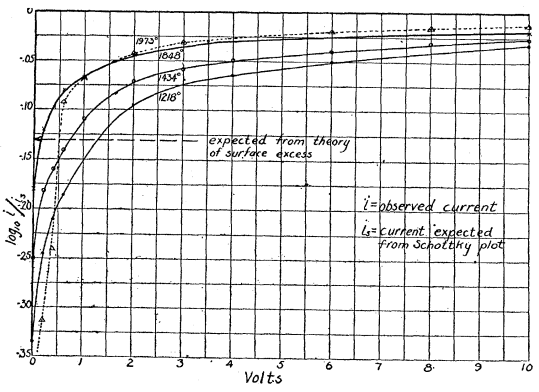

FIG. 14. Departure from Schottky line as a function of accelerating potential.

Observations taken at 1973°K do show the effect of space charge and even those at 1848°K are very slightly influenced near zero field. We also see that the lower the temperature the higher the applied field must be before the Schottky line is followed.

A comparison between Schottky curves obtained with pure tungsten and those observed with thoriated tungsten activated to $Z=1.3$ showed them to be very similar at 1218°K although the current received by the collector was over two million times greater for the thoriated filament. The three curves shown by Fig. 15 may therefore be considered as part of the tungsten family, thus showing quantitatively the extent to which observed Schottky curves actually deviate from the theoretical line as the temperature is lowered.

In seeking an explanation for these experimental observations, it seems obvious that there are only two possibilities. The first is that the transmission properties of a surface considered from a wave-mechanical point of view are very strongly influenced by a change in the form of the potential barrier at the surface. This suggestion seems so far fetched that it can perhaps be eliminated without further consideration. Grant-

[24] Schottky, Physik. Zeits. **15**, 872 (1914). See K. T. Compton and I. Langmuir, Rev. Mod. Phys. **2**, 123 (1930) for short discussion.

* The applied voltage must be corrected by the contact potential to obtain V.

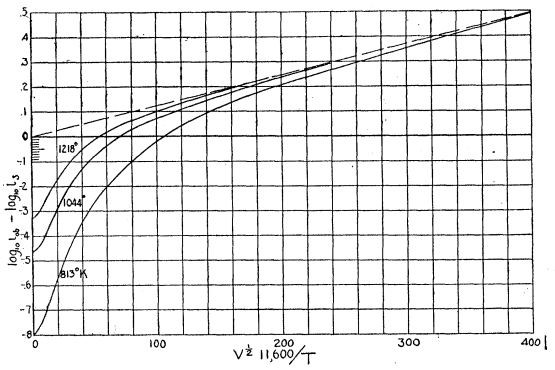

FIG. 15. Schottky plots for thoriated tungsten. $Z=1.3$.

ing this, we are forced to the conclusion that there must be some electrical forces acting on the electrons at distances of the order of 10^{-6} to 10^{-4} cm which are *larger* than the mirror image forces. If the work function of the surface is not uniform but varies perhaps periodically from one crystal facet to another, then the contact potential fields might give rise to the electric fields which would account for the observed effect. Let us call this the "patch effect."

Two other complicating factors of the problem are the effect of field concentration at sharp points and the geometrical effect of surface excess.[25] The first of these would be temperature dependent in the direction observed but the fact that all experimental curves either fit the theoretical curve accurately for high fields or else approach it asymptotically is an indication that field concentration is of secondary importance in this problem. The "surface excess" effect would not be temperature dependent and therefore although this might account for a ten to thirty percent increase in current as the field is increased, it is not as important as the "patch effect" as a possible explanation of the experimental observations.

The sky-line and the patch theory*

No patch theory so far proposed can be applied to the problem of emission as a function of the electric field except in an approximate form as was done by Becker[26] and will also be done below in connection with the "strip theory." In order to demonstrate this, let us consider the problem in terms of the statistics of a perfect gas. We imagine an infinite conductor essentially in a plane and take the Y and Z axes of a coordinate system in this plane with the X axis extending into space. Designate this plane as the A plane. We assume that the work function for electrons is independent of y but varies periodically with z. Consider also a second conducting plane, known as the B plane, parallel to the first at a distance D which is very large compared with the fundamental wave-length of work function differences in the z direction or the distance between similar regions in the first plane. We have "zero field" in the space between these planes when no lines of electric force extend from A to B. There will then be no *net* surface charge on either plane.

Consider the boundaries to be at the temperature T and of such work functions that there is no net flow of electricity from A to B or B to A. The time average of the relative electron densities at all points in this space will be governed by the Boltzmann equation and furthermore over any small region where the change in motive* is small, the time average of the energy or the velocity distribution will be governed strictly by Maxwell's distribution function characterized by the temperature T. The motive must be used in the Boltzmann equation because differences in motive measure the work per unit charge required to move an *electron* from place to place. In the absence of an electric field between A and B, the motive will be constant everywhere except in the neighborhood of A where it will be the sum of the electrostatic potential due to the nonhomogeneous surface and the mirror image potential which, of course, does not satisfy Laplace's equation. If the temperature is low, the electrons

[25] L. Tonks, Phys. Rev. **38**, 1030 (1931).

* Some of the ideas presented here were worked out in collaboration with Dr. Irving Langmuir, to whom the author is greatly indebted. Part of the terminology therefore follows that of Mott-Smith and Langmuir, Phys. Rev. **28**, 727 (1926) and Langmuir and Compton, Rev. Mod. Phys. **3**, 191 (1931).

[26] J. A. Becker, Rev. Mod. Phys. **7**, 95 (1935).

* The term "motive" has been defined by Langmuir as ". . . a scalar quantity whose gradient, in any direction at any point, represents the force-component per unit charge which *acts on an electron or ion*." I. Langmuir and K. H. Kingdon, Proc. Roy. Soc. **A107**, 61 (1925), see p. 68. For an earlier discussion, see I. Langmuir, Trans. Am. Elec. Chem. Soc. **29**, 125, 157 (1916). P. W. Bridgman, reference 21, p. 37, uses the term "electric potential" in contrast to "electrostatic potential" where the former is the equivalent of the "motive" while the latter is a potential which satisfies Poisson's equation.

will be so far apart that one may neglect any interaction between electrons, i.e., we may disregard space-charge effects. We may imagine the phase space as the six-dimensional μ space of an ideal gas and focus our attention on a small region extending over the coordinates $dxdydz$ at (x, y, z) while the extention in momenta may be taken as p_x, p_y, p_z from $-\infty$ to $+\infty$. Since it is assumed that the motive is essentially constant throughout the volume $dxdydz$, we may picture the momentum space alone, remembering that the divisions in this space discussed below are determined by the space coordinates x, y, z.

Let us classify the electrons, whose representative points are seen in the momentum space, as AA electrons, AB electrons, BA electrons, or BB electrons, according to their trajectories. In the absence of space-charge effects there can be no periodic orbits which do not intersect planes A or B. It is evident that for every AB electron there is a corresponding BA electron such that their representative points, in the momentum space, lie diametrically opposite each other. That is, the line joining them will always be bisected by the origin. Thus, within the confines of a certain extended region in the momentum space, we will find all of the AB electrons and an exactly similar region will contain all of the BA electrons with the bounding surface "reflected" in the origin. All of the remaining momentum space will contain the AA and the BB electrons.

The problem of computing the current which would flow from electrode A to B could be solved if we could find some closed surface in the coordinate space between electrodes A and B over which we could correctly bound the above regions in momentum space and thus compute the flux of AB electrons crossing this coordinate surface.

With the system of strips described above, we can easily visualize a hill and valley system. The motive will be a point function depending only on the x and z coordinates. Since we have postulated the work function to be a periodic function of z, we know that we can represent the "surface potential" by a series

$$V(0, z)=\sum_{n=0}^{\infty} a_n \cos n\frac{2\pi z}{z_0}+\sum_{n=0}^{\infty}{}' b_n \sin n\frac{2\pi z}{z_0}. \quad (16)$$

For the purpose of this discussion, let us take only the second term of the first sum, namely, $a\cos 2\pi z/z_0$ as the "surface potential." At $x \gg z_0$ the electrostatic potential must be constant and may be taken as zero. The potential at any point (x, z) must then be

$$V(x, z)=ae^{-2\pi x/z_0}\cos(2\pi z/z_0). \quad (17)$$

since this is a solution to Laplace's equation and fits the boundary conditions. With zero impressed field, the motive will then be

$$M_0(x, z)=ae^{-2\pi x/z_0}\cos(2\pi z/z_0)-\epsilon/4x. \quad (18)$$

Eq. (18) is, of course, not correct for $x<10^{-7}$ cm on account of the failure of the image laws, but it will serve to bring out certain points to follow. Let us now visualize $M_0(x, z)$ as a system of hills constructed on the x, z plane with the altitude at any point (x, z) equal to $M_0(x, z)$.

The form of this surface as seen by an analysis of Eq. (18) has interesting and rather unexpected properties. Differentiating with respect to x and setting the result equal to zero, we have

$$\frac{\partial M_0(x, z)}{\partial x}=0=-\frac{2\pi a}{z_0}\cos\frac{2\pi z}{z_0}e^{-2\pi x/z_0}+\frac{\epsilon}{4x^2}. \quad (19)$$

By substituting $u=2\pi x/z_0$ and rearranging, we find

$$\{(2z_0a/\pi\epsilon)\cos(2\pi z/z_0)\}e^{-u}=1/u^2=Ae^{-u}, \quad (20)$$

where A is defined by this equation. If we express A in terms of u and set $dA/du=0$ we see that for $u=2$, A passes through a minimum value of $e^2/4=1.847$. This means that if A is less than $e^2/4$, Eq. (20) can be satisfied only for $u=\infty$ while if A is greater than $e^2/4$ a *maximum* occurs in the motive as we follow a line of constant z at some value of $x<z_0/\pi$ and a *minimum* comes at $z_0/\pi<x<\infty$.

Thus we see that with zero field all electrons at distances greater than that to the minimum of the motive are accelerated toward the surface A for any finite value of a or z_0. This analysis brings out the fact that even though the "patch" fields may greatly exceed the image field at intermediate distances, the image field finally outlasts the patch field because the latter falls off exponentially with the distance.

If we could solve Eq. (19) for x, we would have an expression by which we could calculate the distance from the plane to the maximum in the motive as a function of z for any given values of a and z_0. These values of x and z could then be substituted into Eq. (18) and the motive along the line of maximum motive could be computed. Since the motive is a function of x and z and is independent of y we see that by the elimination of x between Eqs. (18) and (19) we would have M_0 as a function of z. Let us visualize this as the "sky-line" of the system of "hills" as viewed from a great distance. This "sky-line" intersects the $M_0=0$ contour at $x=z_0/2\pi$ and therefore it is seen to shift to $x=\infty$ and remain constant at $M=0$ for a distance in z approximately equal to $z_0/2$ after which the "sky-line" again returns to $x=z_0/2\pi$. Other contours are intersected at

$$x=z_0/\pi(1+(8M_0z_0/\epsilon\pi+1)^{\frac{1}{2}}). \quad (21)$$

Although all of this discussion has been for the case of zero field, it is possible to determine the motive along the "sky-line" for either accelerating or retarding fields and it is from these values of motive that the emission current is computed using the "sky-line" approximation. According to this approximation, we assume that those electrons escape which leave the surface at a particular value of z with energy $p_x^2/2m$ greater than the sky-line motive at that value of z and that electrons with energy less than this do not escape. The approximation made by Becker[26] in his computation is in reality the same as this one.

The form of the sky-line is shown graphically in Fig. 21 for $Z=0.25$ and $Z=1.3$. The ordinate is determined by z and the abscissa is equal to M_0. Some of the electrons included in the current calculated by this method are most certainly AA and not AB electrons. Other electrons with energy enough to escape, given the proper z component of momentum, will be excluded, while in reality they are AB electrons. Thus, it is not possible to state either the amount or the direction of one's error when the sky-line approximation is used.

There must be a line somewhere over the $M_0(x, z)$ surface at which marbles allowed to roll freely from rest go indeterminately either to A or to B. Defining this as the "marble-shed" line, it will probably be true that practically all electrons crossing this line are AB or BA electrons. If so, it would be a better approximation to compute the flux of electrons across a surface so defined but since it would generally be too difficult a problem to find the marble-shed line, this suggestion serves little purpose. This discussion, it is hoped, brings out the difficulties in the way of a proper solution to the problem, and perhaps shows that we cannot expect to get one in the near future.

The Strip Theory with Accelerating Fields

If Becker's[26] "checker-board" patch theory is correct in principle, then a certain amount of reflection of slow electrons should be expected, as was shown to be experimentally true. It was therefore thought desirable to investigate the properties of his equations in the retarding potential region. A partial examination showed that the labor involved would be so great that it would be just as easy to work out the simpler "strip theory" and then examine its predictions instead of those of the checkerboard patch theory. It is the purpose of this part to work out this theory and make application for both accelerating and retarding potentials.

In the presence of an accelerating field of electric intensity E the motive is given by

$$M=a\cos(2\pi z/z_0)e^{-2\pi x/z_0}-\epsilon/4x-Ex. \quad (22)$$

Using u and A as above and differentiating with respect to u we see that

$$\partial M/\partial u=(\pi\epsilon/2z_0)(-Ae^{-u}+1/u^2-Ez_0^2/\epsilon\pi^2). \quad (23)$$

If we set $\partial M/\partial u=0$, we have an equation relating u and E along the sky-line. In principle, we must solve this equation for u and substitute it into Eq. (22) and thus obtain M_E as a function of E and z along the sky-line. Since this is mathematically impractical we can use the following equations and method to obtain the desired result.

$$M_E=a\cos(2\pi z/z_0)(1+u)e^{-u}-\pi\epsilon/z_0\cdot 1/u, \quad (24)$$

$$E=\epsilon\pi^2/z_0^2u^2-(2\pi a/z_0)\cos(2\pi z/z_0)e^{-u}. \quad (25)$$

To use these equations, one chooses values of u for which E has positive values of a magnitude in the range of interest. Using these same values of u we can compute the corresponding values of M_E. In order to compute the current as a function of E or $E^{\frac{1}{2}}$, as is done here, we choose an arbitrary value of z_0 and an arbitrary set of values of $a\cos 2\pi z/z_0$. For example, we have taken $z_0=5\times10^{-4}$ cm, $a=0.5$ volt, and values of z which give $\cos 2\pi z/z_0$ the values 1, 0.8, 0.6, 0.4, 0.2, and 0 and also the negatives of these values. For each selection of z a curve was plotted giving M_E as a function of $E^{\frac{1}{2}}$ as computed from Eqs. (24) and (25). This step was necessary since it was easier to choose arbitrary values of u and find the corresponding values of M_E and E than it was to take definite values of E and then compute the value of M_E. From the curves, however, the desired M_E values for specific values of $E^{\frac{1}{2}}$ were selected. The sky-line curves were then given by plotting M_E as a function of z for chosen $E^{\frac{1}{2}}$ values. The current was computed by graphically evaluating

$$I_E=I_0\int_0^{z_0}e^{-M_E 11{,}600/T}dz. \tag{26}$$

This method of computation is certainly more accurate than Becker's method of sub-squares, although in principle they are much alike. The constant I_0 is of no particular importance since it is the change in $\log_{10}I_E$ with $E^{\frac{1}{2}}$ which is of interest. We therefore take I_0 as unity.

We notice that Eq. (26) shows that the theoretical curves approach the slope of the mirror image curve for very high fields since in this case $u=\epsilon^{\frac{1}{2}}\pi/z_0E^{\frac{1}{2}}$ and Eq. (26) may be approximated by

$$I_E=I_0\exp\frac{(300)^{\frac{1}{2}}\epsilon^{\frac{1}{2}}E^{\frac{1}{2}}\cdot 11{,}600}{T}$$

$$\int_0^{z_0}\exp\{-(11{,}600\,a/T)\cos(2\pi z/z_0)\}dz \tag{27}$$

for high values of E. In Eq. (27) E is expressed in volts per cm.

The final check between theory and experiment was made easy by the use of the curves of Fig. 16. Here $(\log_{10}I_E-\log_{10}I_S)$ is plotted as a function of a as computed with various values of $E^{\frac{1}{2}}$ for the temperature 1160°K. The constant I_S is defined by the following equation:

$$I_S=I_0\int_0^{z_0}\exp\{-(11{,}600\,a/T)\cos(2\pi z/z_0)\}dz, \tag{28}$$

Table II gives $\log_{10}I_S$ for enough values of $11{,}600\,a/T$ so that an interpolation curve may be constructed for $I_0=$ unity.

In order to find an appropriate value of a to fit a given experimental curve, we determine the

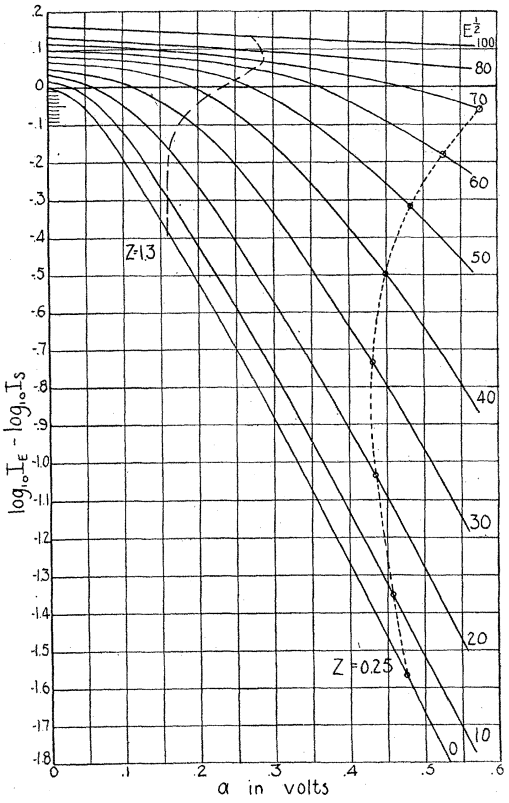

FIG. 16. Chart for computing Schottky curves for $T=1160$°K, using $z_0=5\times10^{-4}$ cm. Dotted line, observed results for $Z=0.25$. Dashed line, observed results for $Z=1.3$.

TABLE II. *Values of $\log_{10}I_S$ for various values of $11{,}600\,a/T$* (see Eq. (28)).

$11{,}600\,a/T$	0.5	1.0	1.5	2.0	2.5	3.0	3.5
$\log_{10}I_S$	.027	.102	.214	.365	.520	.691	.865
$11{,}600\,a/T$	4.0	4.5	5.0	5.5	6.0	6.5	7.0
$\log_{10}I_S$	1.045	1.232	1.426	1.624	1.825	2.025	2.240

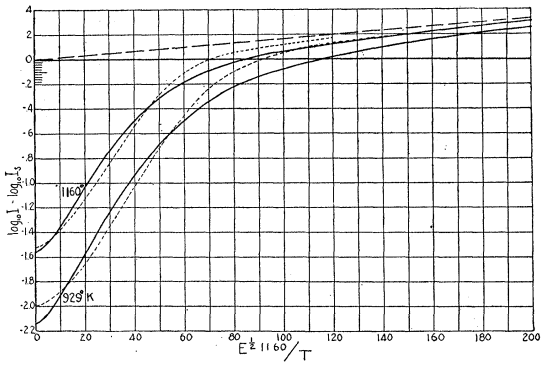

FIG. 17. Computed and experimental Schottky curves for $Z=0.25$. Dotted lines computed with $z=5\times10^{-4}$ cm and $a=0.465$ volt. Asymptotic Schottky line shown dashed.

values of $(\log_{10} i_{ob}-\log_{10} i_S)$ where $\log_{10} i_{ob}$ is the logarithm of the observed current for the values of field specified on Fig. 16. We define $\log_{10} i_S$ as the intercept on the $E^{\frac{1}{2}}=0$ axis of the Schottky line to which the observed Schottky curve is found to be asymptotic. Such Schottky lines are illustrated by Figs. 8, 13 and 15. These values $(\log_{10} i_{ob}-\log_{10} i_S)$ may be located on the corresponding $E^{\frac{1}{2}}$ lines as is shown by the circles which are joined by a dotted line in Fig. 16. The observed data were obtained at 1160°K with the filament activated to $Z=0.25$. For a perfect agreement between theory and experiment, this line would be straight and follow up a constant value of a. On the basis of this curve, however, we choose $a=0.465$ volt as perhaps the best value of a to represent this set of data and read off computed values of $(\log_{10} I_E-\log_{10} I_S)$ which are plotted as a function of $E^{\frac{1}{2}}$ to be compared with the observed values as shown in Fig. 17. The theoretical curve and the experimental one certainly have the same general shape and intersect at two points as they should, since we have two adjustable constants z_0 and a. A more important test is obtained if we compute the curve for a different temperature using the constants thus determined from the 1160°K data and compare this curve with the observed data. This test is also shown in Fig. 17 for here we have the observed and computed curves for 929°K and $Z=0.25$ and have used the values of z_0 and a found most suitable to fit the data observed at 1160°K. The observed points have been omitted from these curves since the accuracy of measurement was so great that all of the points lie accurately on the smooth curves shown.

Fig. 18 summarizes the observed results for a wide range of activation states. The state defined by $Z=0.25$ is thought to be the one for which the deviation from the Schottky mirror image theory is the greatest.

Using these methods, we have determined the most suitable values of a to represent all of the states of activation shown by Fig. 18 and have

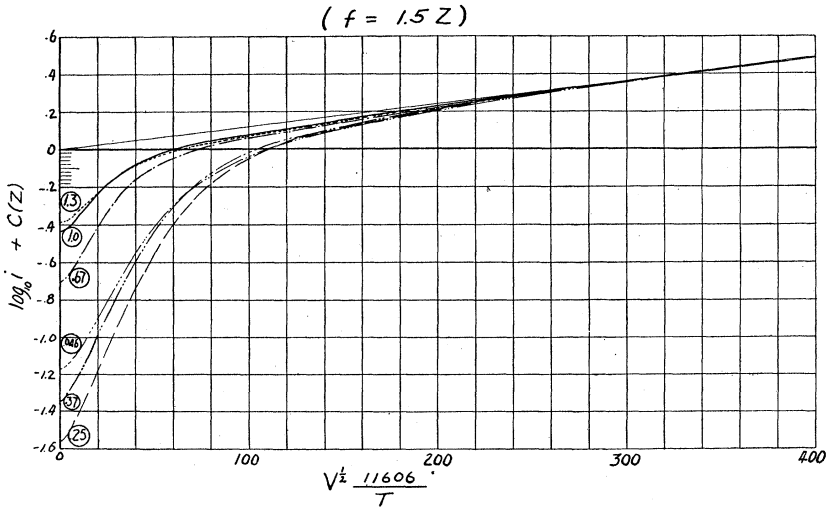

FIG. 18. Observed Schottky curves for six states of activation of a thoriated filament at $T=1160$°K.

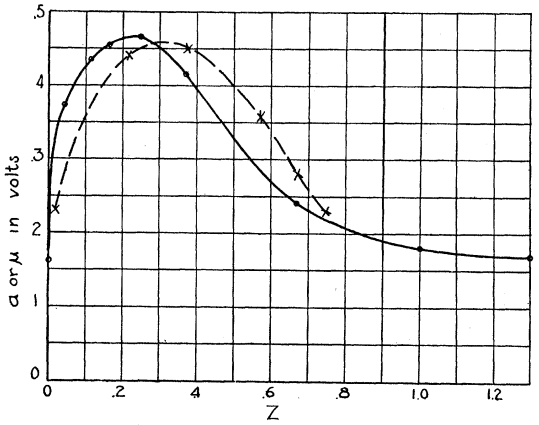

FIG. 19. Dependence of a on the state of activation Z compared with Becker's values of μ shown by solid and dashed lines respectively.

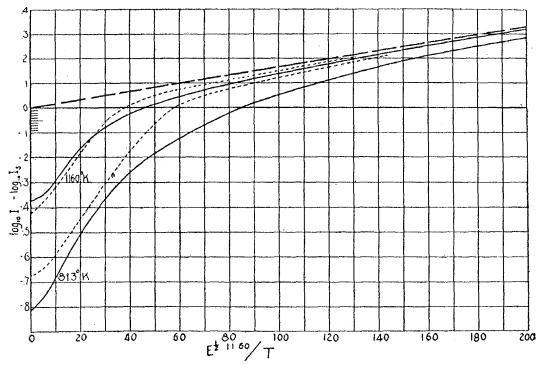

FIG. 20. Computed and observed Schottky plots for $Z=1.3$. $z_0=5\times10^{-4}$ cm and $a=0.17$ volt.

plotted a as a function of Z in Fig. 19. Here also are plotted Becker's[26] values of μ which is the corresponding quantity in his patch theory. It is interesting to note the rather close similarity of the two curves.

As was pointed out above, Schottky curves obtained with $Z=1.3$ are very similar to those obtained with pure tungsten. It is therefore thought desirable to show graphically the comparison between observation and theory for this case. Fig. 20 presents the data for the temperature 1160°K and 813°K.

Again the 1160°K data were used to determine the value of a which was also used to represent the 813°K observations. The agreement as regards the temperature effect is thus seen to be less satisfactory for $Z=1.3$ than for $Z=0.25$. It is

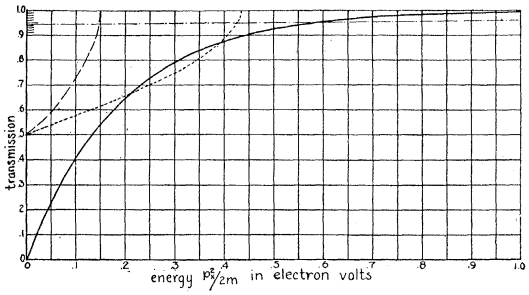

FIG. 21. Surface transmission as function of energy. Solid line for exponential accurately representing observed data. Dotted and dashed lines demanded by strip theory for $Z=0.25$ and $Z=1.3$. Dot-dash for Frank and Young quantum theory.

even more evident in this case that the computed curve approaches the Schottky line too rapidly for the high fields. This difficulty could be partially removed by choosing a smaller value of z_0 but then the rise for low fields would be entirely too slow.

It is easy to see from these curves that an improved theory would introduce narrow regions of low work function surface separated by wide regions of higher work function surface. This could no doubt be worked out by using more terms of Eq. (16), but since a new adjustable constant would come with each term and since there is no way yet available to evaluate these independently, it would not be of much value to show that the experimental curves could be represented very accurately by using a strip or patch theory with many terms.

Influence of strips on retarding potential curves

From the sky-lines computed, with $a=0.46$, $z_0=5\times10^{-4}$ and $a=0.17$, $z_0=5\times10^{-4}$, the effect on the energy distributions to be expected by using retarding potentials was determined. These results are best illustrated by curves showing the "transmission coefficient" of the surface as a function of the energy and comparing it with that obtained directly from experiments using retarding potentials.

The solid curve of Fig. 21 accurately represents the observed data for all states of activation of the thoriated filament and very nearly represents the results for pure tungsten. In the case of tungsten, the slight deviations may have been due to experimental error as pointed

out above. The two curves which result from this strip theory are thus seen to be in definite disagreement with experiment. Again it is not difficult to see that with the narrow regions (order of 10^{-5} cm) of low work function surface separated by wide regions (order of 5×10^{-4} cm) of high work function area, the effect of the strips on the retarding potential side would be greatly reduced and at the same time they would serve to give the large deviations from the Schottky theory which have been known to exist, especially with composite surfaces. If it is reasonable to suppose that such a theory of strips or patches might give a satisfactory explanation for the poor saturation effects for accelerating fields without appreciably influencing the currents predicted as a function of retarding potentials, then we must abandon hope of explaining the observed reflection effects by patches and must look to some "atomic explanation" for the excluded areas or the variable transmission coefficient.

I wish to acknowledge my indebtedness to Mr. N. B. Reynolds and Mr. J. E. Ryan for their careful technical assistance and to my students for many helpful discussions.

JANUARY 1, 1936 PHYSICAL REVIEW VOLUME 49

Negative Atomic Hydrogen Ions

WILLARD H. BENNETT AND PAUL F. DARBY, *Mendenhall Laboratory of Physics, Ohio State University*

(Received October 14, 1935)

Negative atomic hydrogen ions have been directly observed to exist at the heads of striations in discharges in water vapor. The ions appear to form surprisingly readily in these regions of high density of slow electrons, but they are lost very easily by collision.

NEGATIVE ions are supposed to exist in discharges through gases, as necessary for the explanation of the existence of striations[1] as well as for other reasons. They have not been observed there directly, but have been detected and studied in the past at extremely low currents differing greatly from those of the usual kinds of discharge through gases.

In work begun recently at this laboratory, negative atomic hydrogen ions have been observed directly at relatively high densities in the heads of striations in discharges through water vapor, and some information about their properties and behavior in a discharge obtained. The results establish that the ions exist at the heads of striations at high enough densities to play the role assigned them.

METHOD OF OBSERVATION

Various forms of discharge in water vapor were used as sources. In order to analyze the beams obtained through an aperture in the anode of the discharge, an electric lens system was used, shown in Fig. 1. The products from the source came through a sharp-edged aperture in *A*, 1 mm in diameter, and were accelerated by about 1200 volts into *B*. Approaching *C*, which had an accelerating potential of about 16,000 volts, the particles were focused, and going from *C* into *D* they were defocused less, thus producing a real image of the source aperture on the willemite-covered copper screen, *F*. The spot was observed through a screened narrow slot, *E*, and focused by adjustment of the middle electrode on the xylene-alcohol 10-megohm potential divider. A magnetic field from the Helmholtz coils *HH* deflected the particles through a hole in the screen on a collecting electrode, *G*, for measurement. The hole in *F* should be out from the plane of the figure when the coils *HH* are oriented as shown.

A great advantage of the electric lens system used was that when the potential divider was set for focus of the slowest electrons emerging

[1] See Thomson, *Conduction of Electricity Through Gases* (1933), vol. 2, pp. 387ff.